Journal of Power Sources 221 (2013) 172–176

Contents lists available at SciVerse ScienceDirect

Journal of Power Sources

journal homepage: www.elsevier.com/locate/jpowsour

Short communication

Efficient water recirculation for portable direct methanol fuel cells using electroosmotic pumps

Kilsung Kwon, Daejoong Kim*

Department of Mechanical Engineering, Sogang University, Seoul, Republic of Korea

HIGHLIGHTS

- Demonstration of DMFCs integrated with three electroosmotic pumps.
- Efficient water recirculation in air-breathing DMFCs with electroosmotic pumps.
- Significantly low parasitic power ratio of 2.1% for 4 M methanol solution.

ARTICLE INFO

Article history:
Received 4 May 2012
Received in revised form
27 June 2012
Accepted 31 July 2012
Available online 21 August 2012

Keywords:
Active fuel management
Air-breathing direct methanol fuel cell
Water recirculation
Electroosmotic pump
Porous glass frit

ABSTRACT

We present an efficient water recirculation method for air-breathing direct methanol fuel cells (DMFC) by utilizing so-called electroosmotic (EO) pumps. The fuel management system includes three EO pumps for the delivery of methanol solution, pure methanol, and pure water, respectively. Water recirculates from the fuel cell back to the fuel supply stream with the aid of these pump systems. We characterized the performance of the air-breathing DMFC for 2 M and 4 M methanol solutions using a syringe pump and EO pumps, respectively. The DMFC performance is similar for both types of pumps as long as the EO pump operates with the applied voltage of 6 V or higher. The maximum net power density (fuel cell power generation minus pump power consumption) was 50 mW cm^{-2} for 2 M methanol solution and the applied pump potential of 8 V. The minimum parasitic power ratio (pump power consumption divided by fuel cell power generation) was merely 2.1% for 4 M methanol solution and the applied pump potential of 6 V. We successfully demonstrated that the air-breathing DMFC integrated with the EO pumps operated in a stable condition in 1-h galvanostatic measurement.

1. Introduction

Direct methanol fuel cells (DMFCs) are regarded as a promising contender to replace the current battery technology because they offer multiple advantages such as instant recharging (i.e. injecting methanol), high energy density, and simple structure with no moving part [1–7]. Many companies including MTI micro fuel cells, Toshiba, and Samsung advanced institute of technology (SAIT) have developed DMFCs for the application of portable electronic devices [8–10]. There are however still some issues in the commercialization of DMFCs, e.g. their high system cost, low fuel conversion efficiency, and power loss due to methanol crossover [11,12].

Methanol crossover, a permeation of methanol through a membrane, has been identified as an important problem of DMFCs. Numerous studies have been conducted for solving this problem [13,14]. The proposed solutions can be divided into three types: (1) the modification of membranes to reduce methanol crossover [15–17], (2) the development of highly active catalysts [13,18–21], and (3) the use of diluted methanol solutions (1–2 M in active fuel supply and 3–5 M in passive fuel supply) [22–24]. The use of diluted methanol solutions especially has been identified as a common solution to the methanol crossover because of simplicity and compatibility with pre-existing systems. The technique typically includes water recirculation: pure methanol is pumped from the fuel storage, pure methanol is diluted with water, diluted methanol is supplied to a fuel cell, only methanol is used up in the fuel cell, and the leftover water from the fuel cell is re-circulated for methanol dilution. This way, energy density can be increased by storing only pure methanol instead of diluted methanol. The key to this type of system is thus efficient fuel management so that leftover water can be supplied without loss and the flow rate is controlled to maintain the methanol concentration. Recently, various fuel management methods for DMFCs were reviewed by Zhao et al. [25].

* Corresponding author. Tel.: +82 2 705 8644; fax: +82 2 712 0799.
E-mail address: daejoong@sogang.ac.kr (D. Kim).

0378-7753/$ – see front matter © 2012 Elsevier B.V. All rights reserved.
http://dx.doi.org/10.1016/j.jpowsour.2012.07.113

Nomenclature

A	cross-sectional area (m^2)
L	thickness (m)
P	power (W)
Q	flow rate (ml min^{-1})
V_{app}	applied voltage (V)
ε	permittivity of liquid (F m^{-1})
μ	viscosity (Pa s)
σ_∞	ionic conductivity (S m^{-1})
τ	tortuosity (−)
ψ	porosity (−)
ζ	zeta potential (V)

Micropumps that can precisely control flow rate are needed for the fuel delivery or fuel management of portable DMFCs [26–28]. Electroosmotic (EO) pumps are micropumps based on electroosmosis. Electroosmosis refers to the bulk motion of an electrolyte, caused by Coulombic interaction of external electric fields with the charges of a so-called electric double layer (EDL). EO pumps are suitable for DMFC applications because they generate high flow rate and pressure in a small volume and it is easy to control the flow rate by adjusting the voltage [29–35]. One advantage of EO pump-DMFC integration is the removal of electrolysis-originated bubbles (one weakness of EO pumps) simultaneously with carbon dioxide generated by methanol oxidation in DMFCs. Buie et al. recently demonstrated that an EO pump can efficiently deliver diluted methanol solutions (2–8 M) to an air-breathing DMFC [36]. They found that the EO pump consumed only 5% of DMFC power to supply fuel to the DMFC.

In our previous work, we demonstrated that EO pumps can deliver pure methanol and pure water as well as methanol solutions [37]. This suggests a potential application of our EO pumps for water recirculation in DMFCs. In this work, we report an efficient water recirculation scheme for fuel management of the air-breathing DMFC by utilizing three EO pumps.

2. Experimental

The fuel cell we used was an air-breathing fuel cell with the cathode open to the atmosphere. The cathode current collector was in a rib shape with 50% open ratio. The anode flow field has a single serpentine pattern, with the width of 1 mm and the depth of 0.5 mm. A serpentine channel is considered as an appropriate structure for removing carbon dioxide generated at the anode [36]. The anode current collector was fabricated by gold-plated stainless steel. We used a membrane electrolyte assembly (MEA) with the surface active area of 1.4 cm by 1.4 cm (12D-W, BASF). The silicone gaskets with a 0.2 mm thickness were located both at the anode and cathode sides of the MEA. The pure platinum mesh (LS363232, Goodfellow, wire diameter of 0.06 mm) was inserted between the gas diffusion layer (GDL) and the cathode current collector to reduce Ohmic loss. We assembled all these components with bolts and nuts and the tightening pressure was 2 N m, an optimal value found for our setup.

Fig. 1 shows the schematic of the DMFC integrated with the fuel management module (i.e. three EO pumps). We characterized the

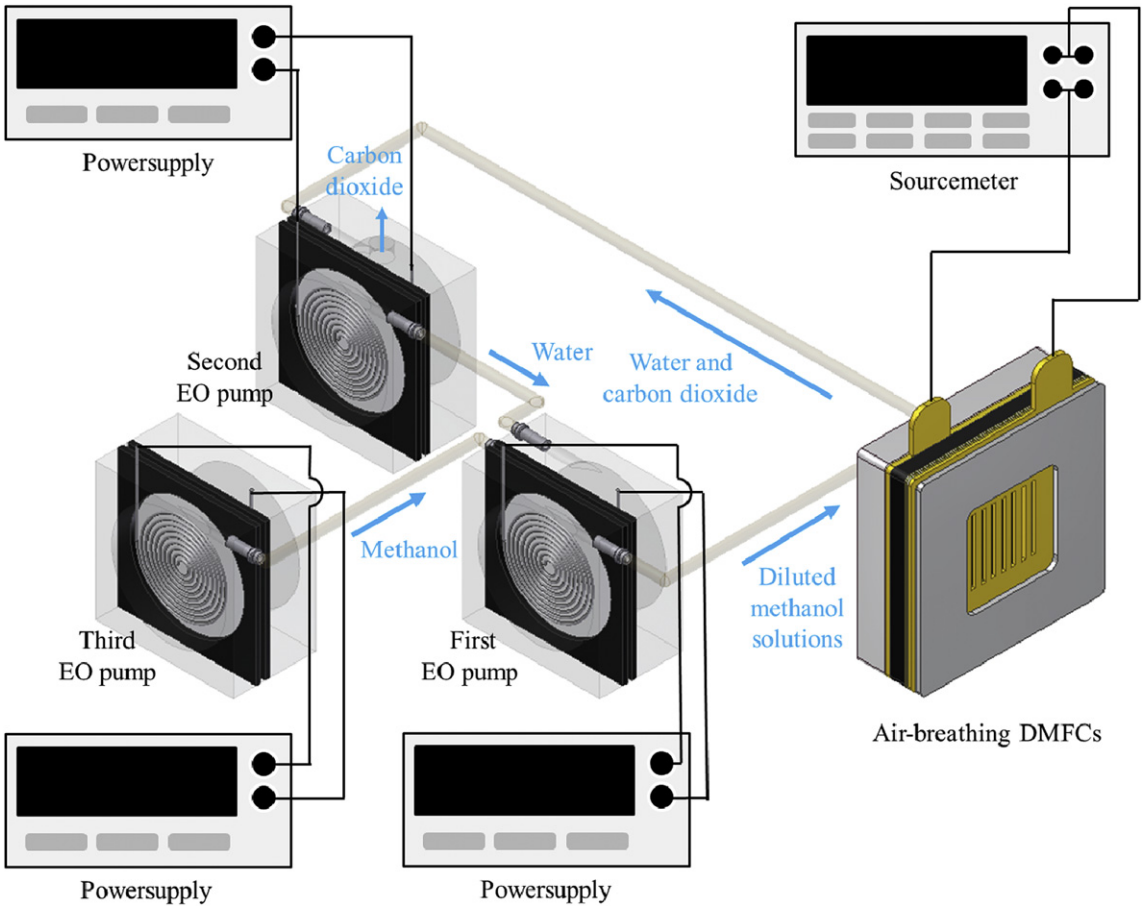

Fig. 1. Schematic of the experimental setup including an air-breathing DMFC, a sourcemeter, three EO pumps, three power supplies, and three multimeters (not shown).

performance of the air-breathing DMFC using a sourcemeter (2410, Keithley). It operated in a four-wire sense mode. We recorded the generated voltage and current signals using the GPIB card and Labview 9.0 (National Instruments). We supplied electrical energy to the EO pumps using DC power supplies (U3606A, Agilent) and measured the consumed power using multimeters (34410A, Agilent). The key component of the EO pumps is borosilicate porous glass frits (ROBU Glassfilter-Geraete GmbH) with the diameter of 1.2 cm and the thickness of 1.5 mm for electroosmotic flow generation. The pumps also include EPDM gaskets for fluid sealing, spiral platinum wires (ϕ 0.3 mm) for electricity application, and methanol-safe PVC liquid reservoirs. The detailed description of EO pumps can be found in our previous paper [37,38].

The working mechanism of fuel management is as follows. The diluted methanol solution is pumped to the DMFC with the first EO pump. The electrochemical reaction occurs in the DMFC, leaving carbon dioxide and leftover water. The carbon dioxide and water are moved to the water reservoir, where carbon dioxide is removed due to buoyancy effect. The second EO pump delivers this degassed water (and a minute amount of un-reacted methanol) to the first pump reservoir. The third pump delivers pure methanol from the fuel storage to the first pump reservoir. In the first pump reservoir, water and methanol are mixed at a given ratio to maintain the preset methanol concentration. This diluted methanol solution is pumped to the fuel cell and the fuel management system finishes its closed loop as such.

We conducted the conditioning of MEAs for the optimal cell performance before the initial use of MEAs. The conditioning procedure is as follows. We hydrated MEAs for 2 h or more using 80 °C hot water and humidified air. After hydration, we streamed the 2 M methanol solution to the anode and dried air to the cathode, respectively, for 12 h or more. We then repeated the DMFC operation under the constant load (potential of about 0.3 V) and measured the polarization curve until the maximum power became nearly constant. We performed the production experiment with a typical procedure. We obtained each polarization curve in a galvanostatic mode. We fixed the current steps at 20 mA and kept each step for 30 s. The total run time was 10 min or more for each case of experiments. We rinsed the DMFC with the methanol solution between the measurements. This rinsing step removed the effect of carbon dioxide in the anode.

3. Results and discussion

We characterized the performance of EO pumps with pure water, pure methanol, and 2 M and 4 M methanol solutions. The working principle and detailed models are reported elsewhere [29,37]. The flow rate in the absence of back pressure is given as $Q \approx -\psi\varepsilon\zeta A V_{app} f/(\tau\mu L)$, where τ, ψ, A, and L are the tortuosity, porosity, cross-sectional area, and thickness of the porous media, respectively. ε and μ are the permittivity and viscosity of liquids and ζ is a so-called zeta potential, which is the characteristic parameter for a given porous material and a solvent. The factor f is a correction factor due to the overlap of so-called electrical double layers [29]. We measured flow rate at different voltages (20, 40, 60, 80, 100 V) and found that flow rate per voltage Q/V_{app} is 17, 11, 9.0, and 9.1 μL min^{-1} V^{-1} for pure water, pure methanol, 2 M methanol solution and 4 M methanol solution, respectively. These values however should be used with caution that the applied voltage can be different from the voltage effective in electroosmosis [29]. The flow rate per voltage Q/V_{app} therefore would be lower than these values especially under the pump voltage of 5 V. We reported the performance of the EO pump for a full range of methanol concentrations in [37].

One useful parameter in this study is the flow rate per power while the power consumption can be obtained by multiplying the applied voltage by the consumed current. It can be theoretically expressed as $Q/P = -\varepsilon\zeta g/(V_{app}\mu\sigma_\infty)$ [36]. Here, σ_∞ is ionic conductivity of liquid and g is another correction factor like the factor f [29]. The flow rate per power is inversely proportional to the applied voltage. Q/P is 3.7, 3.4, 2.8, and 23 mL min^{-1} W^{-1} at 100 V for water, methanol, 2 M methanol solution, and 4 M methanol solution, respectively.

We characterized the performance of the air-breathing DMFC. Fig. 2 shows the polarization curves for (a) 2 M and (b) 4 M methanol solutions. We supplied enough fuel with a fixed flow rate of 100 μL min^{-1} and we maintained the operating temperature around 50 °C. We conducted the experiments with a syringe pump (Pump33, Harvard) as a benchmark case. The open circuit voltage (OCV) with the 4 M solution is lower than with the 2 M solution because of the increased mixed potential, the result of the increased methanol crossover. We observed rather high activation loss by sluggish methanol reaction at low currents during polarization testing. We however did not observe a clear indication of concentration loss in the experiments with the syringe pump. The maximum power density with the syringe pump is 51 mW cm^{-2} at 250 mA cm^{-2} and 46 mW cm^{-2} at 180 mA cm^{-2} for 2 M and 4 M methanol solutions, respectively. The maximum power density is therefore greater with 2 M solution than with 4 M solution in this benchmark experiment.

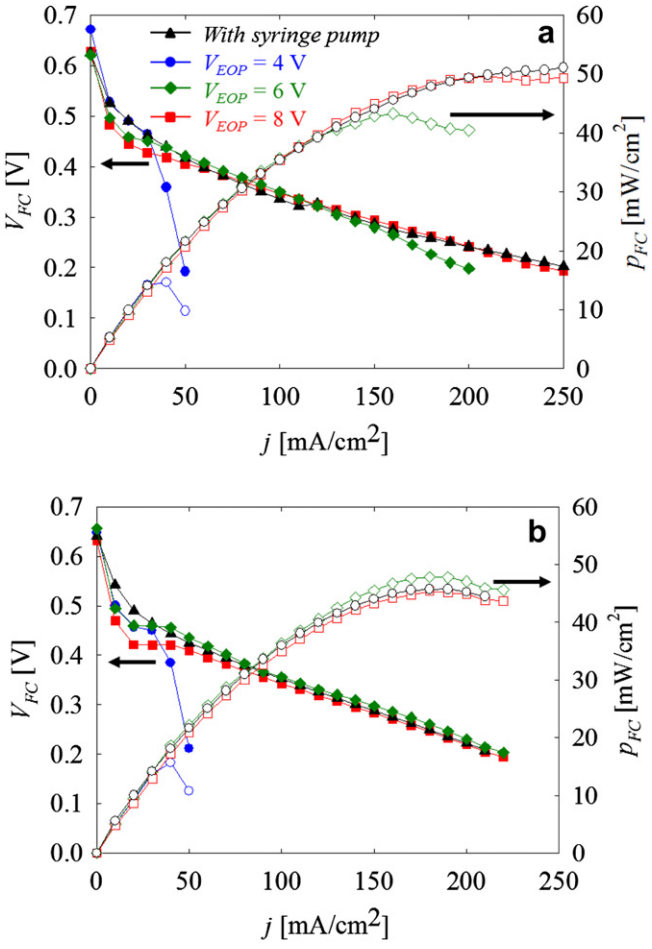

Fig. 2. Polarization and power density curves for (a) 2 M and (b) 4 M methanol solutions.

We characterized the performance of the air-breathing DMFC integrated with the EO pump while we varied the EO pump voltages among 4, 6, and 8 V. The general trend is similar to the benchmark case except for the EO pump voltage of 4 V. The performance with 2 M methanol solution showed the maximum power density (50 mW cm^{-2}) at the EO pump voltage of 8 V. In the experiments with 4 M methanol solution, we observed the maximum power density (48 mW cm^{-2}) at the EO pump voltage of 6 V. This power density with the EO pump is almost the same with the syringe pump that in the benchmark case. When the applied voltage was lowered to 4 V, however, the DMFC voltage steeply falls below 0.2 V around the DMFC current of 50 mA cm^{-2} or higher The DMFC anode is starved of methanol due to the low flow rate at the pump voltage of 4 V.

Fig. 3 shows the net power density (the DMFC power generation minus the EO pump power consumption) against the current density. The net power density curves show a parabolic shape similar to the usual power density curve, except for the cases with the EO pump voltage of 4 V. The reason for the similarity is the low EO pump power consumption, meaning that the net power output is close to the DMFC own power. The maximum net power density is 46.6 mW cm^{-2} at the pump voltage of 8 V for 2 M methanol solution and 45.9 mW cm^{-2} at the pump voltage of 6 V for 4 M methanol solution.

Fig. 4 shows the parasitic power ratio, which is defined as the EO pump power consumption divided by the DMFC power generation.

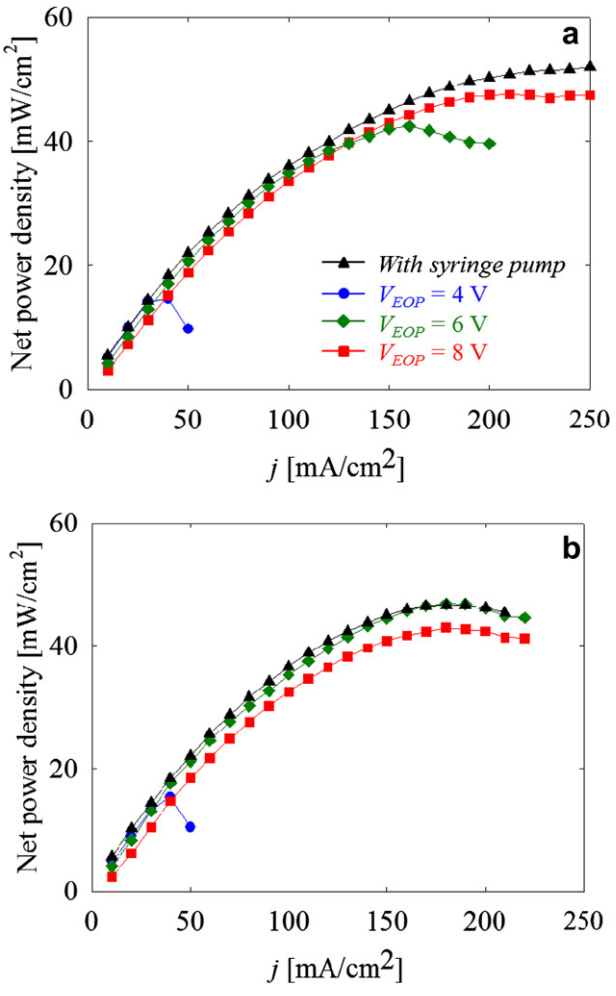

Fig. 3. Net power density (power generation−power consumption) for (a) 2 M and (b) 4 M methanol solutions.

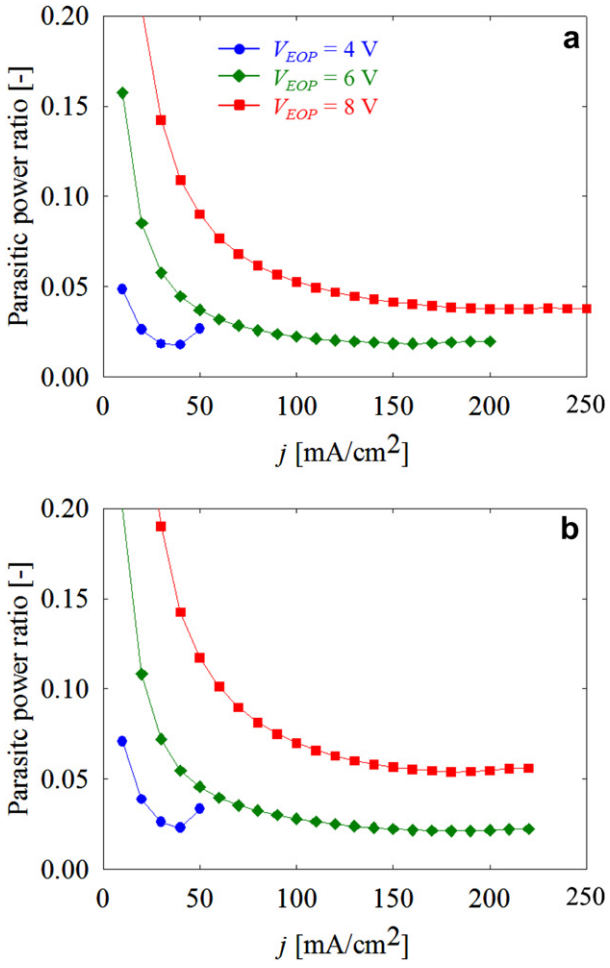

Fig. 4. Parasitic power ratio (power consumption/power generation) for (a) 2 M and (b) 4 M methanol solutions.

This ratio increases with the increasing EO pump voltage and decreases with the increasing DMFC current. It is nearly constant above 100 mA cm^{-2} at the applied voltage of 6 and 8 V for both

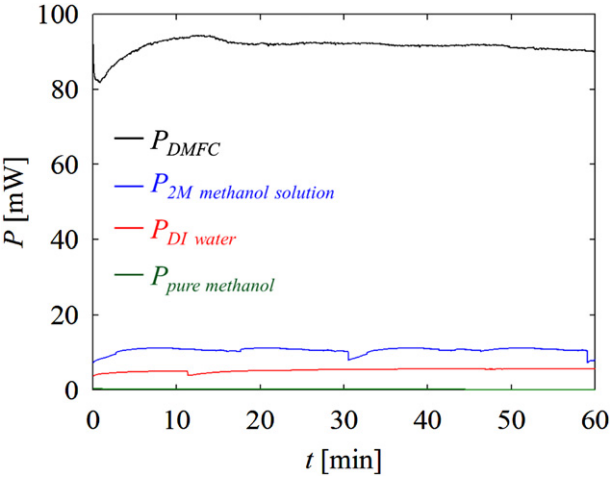

Fig. 5. Time record of power in the air-breathing DMFC integrated with a fuel management module. The DMFC operated at the temperature of 50 °C and the current load of 300 mA. The feed concentration of the DMFC was 2 M methanol solution. The applied EO pump voltages were 8.0, 4.6, and 0.8 V for the pumping of 2 M methanol solution, DI water, and pure methanol, respectively.

methanol solutions. The lowest parasitic power ratio is as low as 2.1% for 4 M methanol solution in this practical operation range.

Fig. 5 shows the 1-h time record of power generation/consumption in our fuel management module. The air-breathing fuel cell operated around the maximum power (2 M methanol solution and current load of 300 mA) for optimal performance. The voltages of EO pumping were at 8, 4.6, and 0.8 V for 2 M methanol solution, DI water, and pure methanol, respectively. We determined these EO pump voltages based on the current load of the DMFC. The power of the air-breathing DMFC slowly ramps up during the initial 5 min and becomes stabilized up to 1 h. The power curves for the EO pumps sometimes show sharp drops and these are due to the overflow of the fuel solutions from the pump reservoirs. This overflow is indebted to the pressure build-up by the generated carbon dioxide. We need to devise a means to remove carbon dioxide efficiently in the future. Most of power consumption is for the supply of 2 M methanol solution and DI water and the power demand for pure methanol is only 0.3 mW. Overall, we achieved the net power of 76 mW and the parasitic power ratio of 14%.

4. Conclusion

We report the performance of EO pumps for pumping pure methanol, pure water, and methanol solutions. We also report the experimental results of the air-breathing DMFC integrated with EO pumps. The DMFC performance with the EO pump is similar to the benchmark performance with the syringe pump as long as the fuel supply is enough at the pump voltage of 6 V or higher. We found that the maximum net power density is 50 mW cm^{-2} with 2 M methanol solution at the EO pump potential of 8 V. We also achieved the minimum parasitic power ratio of 2.1% with 4 M methanol solution at the EO pump potential of 6 V. We also performed 1-h long galvanostatic measurement in the maximum net power condition. The air-breathing DMFC and EO pumps operated stably during this period of time.

The experimental results show that EO pumps can be efficiently applied for fuel management of a DMFC with low power consumption. The current setup however does not include a control scheme to maintain methanol concentration. Although we did not observe any sign of concentration drift during the 1-h long experiment, control over methanol flow rate should be needed for a much longer operation in practical applications. The control scheme would include a sensor for methanol concentration, a pump voltage metering, and feedback control algorithm. The gas-buildup is another issue and a possible simple solution would be a gas trap chamber. The electroosmotic pumps in this paper required the voltages higher than the output voltage of a single cell. For practical use, the pumps should be powered by the fuel cell itself, which means that a fuel cell stack should be used. Efficient recirculation in such a fuel cell stack system should be investigated in the future.

Acknowledgment

This research was supported by the Multiphenomena CFD Engineering Research Center (Grant no. 2009-0093136) through the National Research Foundation of Korea (NRF) funded by the Ministry of Education, Science and Technology.

References

[1] G. Lu, C. Wang, T. Yen, X. Zhang, Electrochim. Acta. 49 (2004) 821–828.
[2] C. Xie, J. Bostaph, J. Pavio, J. Power Sources 136 (2004) 55–65.
[3] G. Lu, C. Wang, J. Fuel Cell Sci. Technol. 3 (2006) 131–136.
[4] S.K. Kamarudin, F. Achmad, W.R.W. Daud, Int. J. Hydrogen. Energy. 34 (2009) 6902–6916.
[5] S.K. Kamarudin, W.R.W. Daud, S.L. Ho, U.A. Hasran, J. Power Sources 163 (2007) 743–754.
[6] Z. Guo, A. Faghri, Int.Commun. Heat Mass. Transfer 35 (2008) 225–239.
[7] T.S. Zhao, C. Xu, Fuel Cells – Direct Alcohol Fuel Cells | Direct Methanol Fuel Cell: Overview Performance and Operational Conditions, in: Jürgen Garche (Ed.), Encyclopedia of Electrochemical Power Sources, Elsevier, Amsterdam, 2009, pp. 381–389.
[8] http://www.mtimicrofuelcells.com/.
[9] http://www.toshiba.co.jp/about/press/2009_10/pr2201.htm.
[10] http://www.sait.samsung.co.kr/.
[11] A. Heinzel, V. Barragan, J.Power Sources 84 (1999) 70–74.
[12] C. Xu, A. Faghri, X. Li, T. Ward, Int. J. Hydrogen. Energy. 35 (2010) 1769–1777.
[13] S.H. Seo, C.S. Lee, Appl. Energy 87 (2010) 2597–2604.
[14] A. Casalegno, P. Grassini, R. Marchesi, Appl. Therm. Engg. 27 (2007) 748–754.
[15] Fang Yong, Miao Ruiying, Wang Tongtao, Wang Xindong, Fang Shibi, Acta Polymerica Sinica (2009) 992–1006.
[16] H. Ahmad, S.K. Kamarudin, U.A. Hasran, W.R.W. Daud, Int. J. Hydrogen. Energy. 35 (2010) 2160–2175.
[17] S. Ren, G. Sun, C. Li, Z. Liang, Z. Wu, W. Jin, X. Qin, X. Yang, J. Memb. Sci. 282 (2006) 450–455.
[18] S. Wasmus, A. Kuver, J. Electroanal. Chem. 461 (1999) 14–31.
[19] H. Liu, C. Song, L. Zhang, J. Zhang, H. Wang, D. Wilkinson, J. Power Sources 155 (2006) 95–110.
[20] Y.M. Alyousef, M.K. Datta, K. Kadakia, S.C. Yao, P.N. Kumta, J. Alloys Compounds 506 (2010) 698–702.
[21] K. Nam, S. Lim, S.K. Kim, S. Yoon, D. Jung, Int. J. Hydrogen. Energy, 37 (2012) 4619–4626.
[22] M. Ravikumar, A. Shukla, J. Electrochem. Soc. 143 (1996) 2601–2606.
[23] R. Chen, T. Zhao, J. Power Sources 152 (2005) 122–130.
[24] B. Bae, B.K. Kho, T. Lim, I. Oh, S. Hong, H.Y. Ha, J. Power Sources 158 (2006) 1256–1261.
[25] T.S. Zhao, W.W. Yang, R. Chen, Q.X. Wu, J. Power Sources 195 (2010) 3451–3462.
[26] T. Zhang, Q. Wang, J. Power Sources 140 (2005) 72–80.
[27] T. Zhang, Q. Wang, J. Power Sources 158 (2006) 169–176.
[28] S. Lee, Y. Kuan, M. Sung, J. Power Sources 196 (2011) 7609–7615.
[29] S. Yao, J. Santiago, J. Colloid. Interface. Sci. 268 (2003) 133–142.
[30] D. Kim, J.D. Posner, J.G. Santiago, Sens. Actuators. A. Phys. 141 (2008) 201–212.
[31] R.F. Probstein, Physicochemical Hydrodynamics, Wiley Online Library, 1995.
[32] S. Yao, D.E. Hertzog, S. Zeng, J.C. Mikkelsen Jr., J.G. Santiago, J. Colloid. Interface. Sci. 268 (2003) 143–153.
[33] Y. Ai, S.E. Yalcin, D. Gu, O. Baysal, H. Baumgart, S. Qian, A. Beskok, J. Colloid. Interface. Sci. 350 (2010) 465–470.
[34] Y. Chen, Y. Hu, Y. Chou, S. Lai, C. Wang, Sens. Actuators. B. Chem. 145 (2010) 575–582.
[35] T. Fabian, R. O'Hayre, S. Litster, F.B. Prinz, J.G. Santiago, J. Power Sources 195 (2010) 3640–3644.
[36] C.R. Buie, D. Kim, S. Litster, J.G. Santiago, Electrochemical Solid State Lett. 10 (2007) B196–B200.
[37] K. Kwon, D. Kim, Sens. Actuators. A. Phys. 166 (2011) 88–93.
[38] K. Kwon, C.W. Park, D. Kim, Sens. Actuators. A. Phys. 175 (2012) 108–115.